Fractionation spares mice from radiation-induced reductions in weight gain but does not prevent late oligodendrocyte lineage side effects

Sage Begolly, Ph.D.[1], **Peter G. Shrager, Ph.D.**[2,3], **John A. Olschowka, Ph.D.**[2], **Jacqueline P. Williams, Ph.D.**[1,4], and **M. Kerry O'Banion, M.D., Ph.D.**[2,5]

[1]Department of Environmental Medicine, University of Rochester School of Medicine & Dentistry, Rochester, NY, USA

[2]Department of Neuroscience, University of Rochester School of Medicine & Dentistry, Rochester, NY, USA

[3]Department of Pharmacology & Physiology, University of Rochester School of Medicine & Dentistry, Rochester, NY, USA

[4]Department of Radiation Oncology, University of Rochester School of Medicine & Dentistry, Rochester, NY, USA

[5]Department of Neurology, University of Rochester School of Medicine & Dentistry, Rochester, NY, USA

Abstract

Purpose—To determine the late effects of fractionated versus single dose cranial radiation on murine white matter.

Methods and Materials—Mice were exposed to 0 Gy, 6×6 Gy, or 1×20 Gy cranial irradiation at 10–12 weeks of age. Endpoints were assessed through 18 months from exposure using immunohistochemistry, electron microscopy, and electrophysiology.

Results—Weight gain was temporarily reduced after irradiation; greater loss was seen after single versus fractionated doses. Oligodendrocyte progenitor cells were reduced early and late after both single and fractionated irradiation. Both protocols also increased myelin g-ratio, reduced the number of nodes of Ranvier, and promoted a shift in the proportion of small, unmyelinated versus large, myelinated axon fibers.

Conclusions—Fractionation does not adequately spare normal white matter from late radiation side effects.

Address correspondence to: M. Kerry O'Banion, 601 Elmwood Ave Box 603, Rochester, NY 14642; Phone: 585-275-5185; Kerry_OBanion@URMC.Rochester.edu.

Summary

Although fractionation reduced cranial radiation-related effects on weight gain, patterns of early and late oligodendrocyte progenitor cell depletion and late white matter pathology and dysfunction were similar following both single and fractionated irradiation. This indicates that fractionation fails to reduce late white matter side effects of radiation in adult mice.

Introduction

The brain is considered a late responding tissue to ionizing radiation (IR) due to the large number of differentiated, post-mitotic cells and the delayed appearance of radiation-related side effects, such as leukoencephalopathy and radiation necrosis (1,2). The use of fractionated radiation has reduced these normal tissue side effects, although significant cognitive deficits are still reported (3,4). Since myelin plasticity is linked to learning (5–8) and working memory (9–11), it is likely that alterations in myelin contribute to the cognitive side effects of radiation exposure. The cells responsible for myelin sheath production, the oligodendrocytes, differentiate from oligodendrocyte progenitor cells (OPCs) and myelinate throughout life (12,13). Because OPCs proliferate and mature in order to maintain the requisite number of myelinating oligodendrocytes, fractionation is unlikely to spare this population, and so the acute effects of radiation on OPCs may contribute to observed late changes in myelin.

We investigated the effects of fractionated versus single dose irradiation on white matter in a murine model of radiotherapy to determine whether fractionation spares radiation-induced myelin dysfunction. Adult mice were exposed to 0 Gy, 6×6 Gy, or 1×20 Gy radiation and OPC numbers, myelin g-ratio, nodes of Ranvier, and electrophysiology were used to assess the white matter response through 18 months from exposure. Direct comparison of single versus fractionated radiation schedules enabled us to determine the radiation paradigm contribution to the severity of side effects.

Methods and Materials

Animals

All animal procedures were approved by the University of Rochester Committee on Animal Resources prior to experimentation. Pdgfrα-CreER^{T2}:Rosa26R-YFP mice (13) were housed in temperature (23 ± 3°C) and light (12:12hr light:dar k) controlled rooms with free access to chow and water. Fifty-two male and 45 female mice were used and sexes were balanced across analyses.

Irradiation procedure

Irradiations were performed using a ^{137}Cs source with a 5 mm×12.2 cm collimator at a dose rate of 119–121 cGy/min, with the beam targeted to the center of the brain. All mice were anesthetized with 100 mg/kg ketamine/10 mg/kg xylazine. Irradiated animals were placed supine on the collimator; 6 fractions of 6 Gy were delivered on Monday, Wednesday, and Friday for 2 weeks or a single 20 Gy dose at the end of the second week. Based on our hypothesis that OPCs are radiosensitive and alterations in the OPC population may

contribute to late changes in myelin, the fraction dose was calculated using an α/β ratio of 10 so that the biologically effective dose (BED) was 60 Gy_{10} for the 20 Gy irradiation and 57.6 Gy_{10} for the fractionated exposures. Animals were sacrificed at 3 weeks, 6 or 18 months following the final radiation exposure. Animal weights were recorded every 4 weeks beginning 3–5 months from exposure. Sex distributions for groups at each time point were: 3 week (2 F/2 M); 6 month (6–7 F/6–9 M); 18 month (6–7 F/8–9 M). For all endpoints, sexes were pooled if no differences were found by 2-way ANOVA (Supp. Fig. 1–4).

Tissue processing and immunohistochemistry

Animals were deeply anesthetized with ketamine/xylazine before transcardial perfusion with 0.15 M phosphate buffer (PB) containing 0.5% w/v sodium nitrite and 2 IU/ml heparin. Three week time point animals were then perfused with 4% paraformaldehyde (PFA) and brains were submerged in 4% PFA at 4°C for 2 hours, equilibrate d in 30% sucrose, and frozen in isopentane. Brains from 6 and 18 month animals were flushed with PB, removed and bisected along the midline. The right hemispheres were immersed in 4% PFA at 4°C for 24 hours, equilibrated in 30% sucrose overnight, frozen in isopentane, and stored at −80°C. All fixed brains were sectioned at 30 μm on a sliding microtome and stored at −20°C in cry oprotectant.

Tissue sections were washed in 0.15 M PB, blocked with 3–10% normal serum (Vector), and incubated in primary antibody as follows: Goat anti-PDGFRα (R&D Systems #AF1062) 1:1000; goat anti-Ankyrin G (Santa Cruz #sc-31778) 1:2000; rabbit anti-Caspr (Abcam #ab34151) 1:3000. Invitrogen Alexa Fluor secondary antibodies were diluted 1:800. Sections were coverslipped with Prolong Gold Antifade Mountant (Invitrogen). Images were acquired using a Zeiss Axioplan IIi microscope, Sensicam QE camera (Cooke), and Slidebook software version 6 (Intelligent Imaging) or using an Olympus FV1000 confocal microscope. Between 2 and 4 images per animal per endpoint were quantified with the observer blinded to sample identity either by hand-counting (PDGFRα+ OPCs, 3 weeks post-IR) or using ImageJ (NIH) macros (PDGFRα+ OPCs, 18 months post-IR and Ankyrin G+ nodes of Ranvier). To create and validate the macros, select images were hand-counted and compared to ImageJ outputs. Additionally, select masks were compared to original images to further confirm count accuracy. Prism 6 (GraphPad) was used for graphing and statistical analyses.

Electron microscopy

Two-3 males and 3 females per radiation group were anesthetized with ketamine/xylazine and perfused with fixative comprised of 2% PFA, 2.5% glutaraldehyde, 50% 0.1 M sodium cacodylate buffer, 6.8% sucrose, and 38.7% water. Brains were removed, submersion fixed for 1 hour, and cut into 1 mm thick sections using a mouse brain Acrylic Matrice (Braintree Scientific #BS-A 5000C). Sections were fixed for at least 24 hours at 4°C, blocked to areas containing the corpus callosum, and osmicated, stained, dehydrated, embedded in resin, and ultrathin sectioned by the Electron Microscopy Core. At least 3 images per animal were captured at 10,000× magnification. Each image was divided into a grid containing 60 same-size boxes, randomly offset, and 6 of these were chosen at random for quantification,

resulting in the analysis of 50–174 axons per animal. ImageJ (NIH) was used for determination of perimeter-based g-ratio (axon perimeter/myelin perimeter).

Electrophysiology

Artificial cerebrospinal fluid (aCSF) contained: 125 mM NaCl, 2.5 mM KCl, 1.25 mM NaH_2PO_4, 25 mM Glucose, 25 mM $NaHCO_3$, 2.5 mM $CaCl_2$ and 1.3 mM $MgCl_2$, and was saturated with 95% O_2/5% CO_2. Mice (4–6 females and 4–6 males per dose per time point) were decapitated and brains were removed, submerged in ice cold aCSF, and cut into 400 μm coronal sections on a vibratome. Sections were incubated for at least an hour in aCSF at room temperature, then placed in a temperature-controlled chamber at 37°C. Electrophysiological recordings across the corpus callosum were performed in a Faraday cage to minimize noise interference and analyzed as described (14). Constant current stimuli (1.3–1.5 mA/ 50 μsec) were delivered through metal bipolar electrodes and recorded using aCSF-filled glass pipettes with resistances of 50–80 KΩ. Records at 3 to 5 interelectrode distances from 0.5 to 1.2 mm were taken to determine the conduction velocity of large, myelinated axons (peak N1) and small, unmyelinated axons (peak N2), as well as the N2/N1 amplitude ratio. Peak amplitudes and conduction times were analyzed by fitting with a third order polynomial, setting the derivative to zero, and calculating the extremum from the resulting quadratic equation. Fits were monitored on the oscilloscope screen. Based on the D'Agostino-Pearson normality test, data was analyzed by 1-way ANOVA or Kruskal-Wallis tests. Outliers (> 2 SD from the mean) were removed as needed.

Results

Weight gain

Radiation-induced reductions in weight gain have been noted in mice (15) and rats (16). Therefore, we assessed weight gain through 78 weeks from radiation exposure. Because starting weights differ between males and females, we analyzed them separately. Analyzing all animals that survived through the end of the experiment revealed that radiation ($F_{(2,42)}$=9.331, p=0.004) and time from exposure ($F_{(14,588)}$=50.37, p<0.0001) significantly affected weight for female mice, with a significant interaction ($F_{(28,588)}$=7.8, p<0.0001) (Fig. 1A). Similarly, a significant effect of radiation dose ($F_{(2,49)}$=19.25, p<0.0001), time ($F_{(14,686)}$=28,63, p<0.0001), and interaction ($F_{(28,686)}$=3.03, p<0.0001) was found for male mice (Fig. 1B). In both female and male mice, 1×20 Gy significantly reduced weight gain compared to unirradiated controls (p<0.001 and p<0.0001, respectively) while no difference was seen between 0 Gy and 6×6 Gy irradiated animals. Additionally, the difference between 6×6 Gy and 1×20 Gy irradiated animals was statistically significant in both female (p<0.01) and male (p<0.001) mice. This suggests that fractionation spared mice from IR-induced reductions in weight gain.

Oligodendrocyte progenitor cell numbers

Because OPCs are the progenitors to myelinating oligodendrocytes, we assessed density of PDGFRα+ OPCs at 3 weeks and 18 months from radiation exposure (Fig. 2). Density of OPCs was reduced at both 3 weeks ($F_{(2,9)}$=38.49, p<0.0001) and 18 months ($F_{(2,44)}$=24.62, p<0.0001) from exposure (Figs. 2B, 2C). This suggests that there was a

sustained depletion of OPCs following radiation, and that this depletion was not spared by fractionation.

Myelination

To determine the impact of radiation on myelin, we used electron microscopy of corpus callosum cross sections to investigate myelin ultrastructure and the degree of callosal myelination. Qualitatively, myelin appeared normal with compact lamellae and no signs of demyelination (Fig. 3A). The g-ratio (axon perimeter/myelin perimeter) can be used to determine the thickness of myelination, with a smaller g-ratio representing a greater amount of myelin per axon. The average g-ratio was not changed at 6 months ($F(2,14)=0.2949$, $p=0.7474$) (Fig. 3B), but was increased in irradiated animals at 18 months from exposure ($F(2,15)=8.435$, $p=0.0035$) (Fig. 3D). When g-ratio was plotted versus axon caliber there was excellent overlap between irradiated animals and controls at 6 months (Fig. 3C); however, at 18 months radiation increased g-ratio primarily in larger diameter axons (Fig. 3E). It therefore appeared that radiation caused a delayed reduction in the amount of myelin per axon, in a size-dependent manner, without evidence of frank demyelination.

White matter function assessment

Proper protein clustering at nodes of Ranvier is linked to myelination (17,18) and can affect axonal signal transduction. In order to identify nodal regions we labeled Ankyrin G, a protein that is responsible for linking sodium channels to the cytoskeleton and is a reliable marker for nodal gaps (19,20), and also Caspr/NCP1, a protein that is localized to paranodal junctions and required for proper organization of paranodal myelin loops (21). Qualitatively, no abnormalities were seen in Ankyrin G and Caspr distribution at nodes of Ranvier in irradiated versus nonirradiated mice at 18 months from exposure (Fig. 4A). While the density of Ankyrin G+ nodes was not altered by radiation exposure at 6 months ($F(2,37)=1.111$, $p=0.3398$) (Fig. 4B), radiation significantly reduced the density of Ankyrin G+ nodes at 18 months ($F(2,43)=7.509$, $p=0.0016$) (Fig. 4C). This suggests a delayed reduction in nodes of Ranvier after radiation exposure.

Myelin wrapping (22), proper assembly of proteins at nodes of Ranvier (23), and axon diameter (24) allow for salutatory conduction and rapid signal transmission. Deficits in myelination can lead to delays or a complete block of conduction. To investigate myelin function, we performed extracellular electrophysiological recordings, assessing interhemispheric signal transmission across the corpus callosum (Fig. 5A). Records typically had two negative peaks: N1, representing fast conducting myelinated axons, and N2, derived from unmyelinated fibers (14). We measured velocities of these two components, and also computed the ratio of the N2 to N1 peak amplitudes (Fig. 5B). At 6 months from radiation exposure, Kruskal-Wallis test showed no difference in N1 velocity (KW stat=2.752 $p=0.2525$) (Fig. 5C) or N2 velocity (KW stat=0.9166, $p=0.6324$) (Fig. 5D) among groups. However, the N2/N1 amplitude ratio was significantly affected by radiation (KW stat=7.8, $p=0.0202$) (Fig. 5E). Dunn's multiple comparisons test showed that 1×20 Gy IR specifically enhanced the N2/N1 ratio at 6 months from exposure. Eighteen months from exposure, the N1 velocity ($F(2,27)=2.735$, $p=0.0829$) and the N2 velocity (KW stat=0.6068, $p=0.7383$) were still unchanged by radiation dose (Figs. 5F, 5G, respectively). However, radiation

increased the N2/N1 ratio (KW stat=9.401, p=0.0091) (Fig. 5H) and Dunn's multiple comparisons test revealed that both 6×6 Gy and 1×20 Gy radiation exposure significantly increased the N2/N1 ratio. These data suggest that the contribution of myelinated axons to conduction relative to that of unmyelinated fibers decreased due to cranial radiation.

Discussion

Current thinking in radiation biology supports the notion that fractionation reduces the normal tissue side effects of radiotherapy in late responding tissues. However, cognitive dysfunction and white matter damage are evident even when fractionation is used, both clinically and in animal models. Therefore, we directly compared the long-term effects of single dose and fractionated radiation on oligodendrocyte lineage endpoints at 6 and 18 months. Additionally, in order to monitor the effects of our cranial radiation protocols on general health, we recorded animal weights. Single dose irradiation caused a marked reduction in weight gain in both sexes through 18 months of exposure. In contrast, mice exposed to fractionated radiation showed no significant difference in weight gain relative to controls. While some reduced weight gain may have been associated with salivary gland dysfunction and the associated overgrowth of teeth, excess tooth growth occurred in all radiation groups. Radiation has been linked to anorexia in humans (25), but since we did not track food consumption, no conclusions can be drawn regarding the contribution of anorexia to the differences in weight gain. Hypothalamic neurogenesis may regulate eating behavior and weight loss in mice (26). However, neurogenesis in other brain areas is susceptible to radiation doses as low as 5 Gy (27); thus, it is unlikely that our fractionated paradigm would have sufficiently spared hypothalamic neurogenesis to contribute to the weight gain differences. Another possible cause for disparate weight gain is hormonal abnormalities due to hypothalamic irradiation. In humans, cranial irradiation impairs hypothalamic-pituitary function (28,29). Rats show reduced growth hormone and IGF-1 levels after cranial IR and reduced pituitary weight is associated with impairments in weight gain (16). Although investigation of hormone levels was not within the scope of this study, it is possible that radiation-induced hormonal disturbances occurred to a greater degree in single dose irradiated animals. Interestingly, reductions in IGF-1 levels associated with weight gain impairment in irradiated rats (16) could also affect OPC behavior, as IGF-1 promotes OPC cell cycle progression and maturation (31).

In order to confirm that OPCs are reduced by radiation exposure, we assessed PDGFRα+ OPC numbers at 3 weeks and 18 months from exposure. OPC numbers were reduced after both single and fractionated radiation, early and long-term, in agreement with other studies (32,33). New myelin is formed throughout life in rodents (34–36), while white matter volume increases to age 40 and then declines in humans (37). A deficit in OPCs could impact continued myelination or remyelination of demyelinated axons through reduced OPC differentiation into myelinating oligodendrocytes. Therefore, electron microscopy was used to assess myelin g-ratio and ultrastructure at 6 and 18 months from single dose and fractionated radiation exposure. Qualitatively, no abnormalities were seen in the myelin of irradiated animals. However, the perimeter-based g-ratio was increased at 18 months after radiation exposure, independent of the radiation paradigm. Because myelin integrity appeared normal, this likely represents a reduction in addition of new myelin during

adulthood in irradiated animals rather than a demyelinating phenotype. In addition to an increased g-ratio, we observed reduced density of Ankyrin G+ nodes of Ranvier at 18 months following both radiation protocols. Internode length has been shown to decrease with normal aging, suggesting myelin turnover and remyelination (38). Therefore, the reduced density of nodes seen after radiation exposure may also represent a decrease in adult myelination.

Compound action potentials across the corpus callosum were measured in order to determine whether these myelin-related alterations could affect white matter function. No change in conduction velocity in either component (N1, N2) was seen at 6 or 18 months after radiation exposure. In principle, an increase in g-ratio should lead to a decrease in conduction velocity. However, as was seen in Fig. 3, the increase in g-ratio was axon size dependent, with only the larger caliber axons affected. Our resolution of the N1 signal at 37°C was limited by the recording distance, and we were unable to measure independently the velocity of the faster (largest) fibers. Thus, while the average velocity, as measured from the N1 peak, was not significantly altered, there may have been changes in specific classes of axons. Moreover, following radiation, the contribution of small unmyelinated fibers to conduction relative to that of large myelinated axons increased, again suggesting a reduction in *de novo* myelination. While myelination should occur throughout life, a sustained depletion of OPCs could reduce the addition of new myelin to previously unmyelinated axons, resulting in a reduction in the proportion of myelinated axons over time.

Our data indicate that the two radiation protocols elicited similar degrees of normal tissue damage, suggesting that conventional fractionation regimens do not spare the murine CNS from sustained OPC depletion, reduced myelination, or alterations in signal conduction. Therefore, with respect to white matter endpoints, alternatives to low dose, prolonged fractionation schedules, such as hypofractionated stereotactic radiotherapy (HSRT), can be considered because of the lack of sparing following conventional practice. In addition, since it appears that fractionation will not reduce late oligodendrocyte lineage-associated side effects, these studies indicate that reducing the volume of the brain exposed to radiation is necessary to minimize late normal white matter damage, offering bench-level support for brain tumor radiosurgery protocols. Clinically, HSRT has been shown to be as effective as whole brain radiation with a stereotactic radiosurgery boost in terms of tumor control and survival (39,40). Moreover, in addition to effective tumor control with HSRT, reduced toxicity has also been suggested in patients with brain metastases (41). These studies, in agreement with our data, suggest that prolonged fractionation paradigms offer no significant benefit to brain tumor patients. Most importantly, the similarities between the acute and late responses following single versus fractionated irradiation in our endpoints justified our use of a high α/β ratio for the BED calculations. This suggests that clinicians should do the same when considering altering fractionation protocols since white matter endpoints are at risk despite their late appearance.

Supplementary Material

Refer to Web version on PubMed Central for supplementary material.

Acknowledgments

References

1. Correa DD, Shi W, Abrey LE, et al. Cognitive functions in primary CNS lymphoma after single or combined modality regimens. Neuro Oncol. 2012; 14:101–108. [PubMed: 22013168]

2. Surma-aho O, Niemela M, Vilkki J, et al. Adverse long-term effects of brain radiotherapy in adult low-grade glioma patients. Neurology. 2001; 56:1285–1290. [PubMed: 11376174]

3. Correa DD, DeAngelis LM, Shi W, et al. Cognitive functions in survivors of primary central nervous system lymphoma. Neurology. 2004; 62:548–555. [PubMed: 14981169]

4. Harder H, Holtel H, Bromberg JE, et al. Cognitive status and quality of life after treatment for primary CNS lymphoma. Neurology. 2004; 62:544–547. [PubMed: 14981168]

5. Sampaio-Baptista C, Khrapitchev AA, Foxley S, et al. Motor skill learning induces changes in white matter microstructure and myelination. J Neurosci. 2013; 33:19499–19503. [PubMed: 24336716]

6. Bengtsson SL, Nagy Z, Skare S, et al. Extensive piano practicing has regionally specific effects on white matter development. Nat Neurosci. 2005; 8:1148–1150. [PubMed: 16116456]

7. Scholz J, Klein MC, Behrens TE, et al. Training induces changes in white-matter architecture. Nat Neurosci. 2009; 12:1370–1371. [PubMed: 19820707]

8. Schlegel AA, Rudelson JJ, Tse PU. White matter structure changes as adults learn a second language. J Cogn Neurosci. 2012; 24:1664–1670. [PubMed: 22571459]

9. Takeuchi H, Sekiguchi A, Taki Y, et al. Training of working memory impacts structural connectivity. J Neurosci. 2010; 30:3297–3303. [PubMed: 20203189]

10. Lee B, Park JY, Jung WH, et al. White matter neuroplastic changes in long-term trained players of the game of "Baduk" (GO): a voxel-based diffusion-tensor imaging study. Neuroimage. 2010; 52:9–19. [PubMed: 20394826]

11. Takeuchi H, Taki Y, Sassa Y, et al. Verbal working memory performance correlates with regional white matter structures in the frontoparietal regions. Neuropsychologia. 2011; 49:3466–3473. [PubMed: 21906608]

12. Psachoulia K, Jamen F, Young KM, et al. Cell cycle dynamics of NG2 cells in the postnatal and ageing brain. Neuron Glia Biol. 2009; 5:57–67. [PubMed: 20346197]

13. Rivers LE, Young KM, Rizzi M, et al. PDGFRA/NG2 glia generate myelinating oligodendrocytes and piriform projection neurons in adult mice. Nat Neurosci. 2008; 11:1392–1401. [PubMed: 18849983]

14. Reeves TM, Phillips LL, Povlishock JT. Myelinated and unmyelinated axons of the corpus callosum differ in vulnerability and functional recovery following traumatic brain injury. Exp Neurol. 2005; 196:126–137. [PubMed: 16109409]

15. Moravan MJ, Olschowka JA, Williams JP, et al. Cranial irradiation leads to acute and persistent neuroinflammation with delayed increases in T-cell infiltration and CD11c expression in C57BL/6 mouse brain. Radiat Res. 2011; 176:459–473. [PubMed: 21787181]

16. Forbes ME, Paitsel M, Bourland JD, et al. Systemic effects of fractionated, whole-brain irradiation in young adult and aging rats. Radiat Res. 2013; 180:326–333. [PubMed: 23952575]

17. Tanaka H, Ma J, Tanaka KF, et al. Mice with altered myelin proteolipid protein gene expression display cognitive deficits accompanied by abnormal neuron-glia interactions and decreased conduction velocities. J Neurosci. 2009; 29:8363–8371. [PubMed: 19571127]

18. Coman I, Aigrot MS, Seilhean D, et al. Nodal, paranodal and juxtaparanodal axonal proteins during demyelination and remyelination in multiple sclerosis. Brain. 2006; 129:3186–3195. [PubMed: 16766541]

19. Dzhashiashvili Y, Zhang Y, Galinska J, et al. Nodes of Ranvier and axon initial segments are ankyrin G-dependent domains that assemble by distinct mechanisms. J Cell Biol. 2007; 177:857–870. [PubMed: 17548513]

20. Komada M, Soriano P. [Beta]IV-spectrin regulates sodium channel clustering through ankyrin-G at axon initial segments and nodes of Ranvier. J Cell Biol. 2002; 156:337–348. [PubMed: 11807096]

21. Bhat MA, Rios JC, Lu Y, et al. Axon-glia interactions and the domain organization of myelinated axons requires neurexin IV/Caspr/Paranodin. Neuron. 2001; 30:369–383. [PubMed: 11395000]

22. Vabnick I, Shrager P. Ion channel redistribution and function during development of the myelinated axon. J Neurobiol. 1998; 37:80–96. [PubMed: 9777734]

23. Brill MH, Waxman SG, Moore JW, et al. Conduction velocity and spike configuration in myelinated fibres: computed dependence on internode distance. J Neurol Neurosurg Psychiatry. 1977; 40:769–774. [PubMed: 925697]

24. Hutchinson NA, Koles ZJ, Smith RS. Conduction velocity in myelinated nerve fibres of Xenopus laevis. J Physiol. 1970; 208:279–289. [PubMed: 5500723]

25. Van Cutsem E, Arends J. The causes and consequences of cancer-associated malnutrition. Eur J Oncol Nurs. 2005; 9(Suppl 2):S51–S63. [PubMed: 16437758]

26. Rojczyk-Golebiewska E, Palasz A, Wiaderkiewicz R. Hypothalamic subependymal niche: a novel site of the adult neurogenesis. Cell Mol Neurobiol. 2014; 34:631–642. [PubMed: 24744125]

27. Zou Y, Corniola R, Leu D, et al. Extracellular superoxide dismutase is important for hippocampal neurogenesis and preservation of cognitive functions after irradiation. Proc Natl Acad Sci U S A. 2012; 109:21522–21527. [PubMed: 23236175]

28. Huang TS, Chen ST, Lui LT, et al. Early effects of cranial irradiation on hypothalamic pituitary function. J Formos Med Assoc. 1990; 89:541–547. [PubMed: 1979595]

29. Lam KS, Tse VK, Wang C, et al. Early effects of cranial irradiation on hypothalamic-pituitary function. J Clin Endocrinol Metab. 1987; 64:418–424. [PubMed: 3818886]

30. Joppa MA, Gogas KR, Foster AC, et al. Central infusion of the melanocortin receptor antagonist agouti-related peptide (AgRP(83–132)) prevents cachexia-related symptoms induced by radiation and colon-26 tumors in mice. Peptides. 2007; 28:636–642. [PubMed: 17204351]

31. Min J, Singh S, Fitzgerald-Bocarsly P, et al. Insulin-like growth factor I regulates G2/M progression through mammalian target of rapamycin signaling in oligodendrocyte progenitors. Glia. 2012; 60:1684–1695. [PubMed: 22836368]

32. Irvine KA, Blakemore WF. A different regional response by mouse oligodendrocyte progenitor cells (OPCs) to high-dose X-irradiation has consequences for repopulating OPC-depleted normal tissue. Eur J Neurosci. 2007; 25:417–424. [PubMed: 17284182]

33. Panagiotakos G, Alshamy G, Chan B, et al. Long-term impact of radiation on the stem cell and oligodendrocyte precursors in the brain. PLoS One. 2007; 2:e588. [PubMed: 17622341]

34. Sturrock RR. Myelination of the mouse corpus callosum. Neuropathol Appl Neurobiol. 1980; 6:415–420. [PubMed: 7453945]

35. Yates MA, Juraska JM. Increases in size and myelination of the rat corpus callosum during adulthood are maintained into old age. Brain Res. 2007; 1142:13–18. [PubMed: 17300760]

36. Nunez JL, Nelson J, Pych JC, et al. Myelination in the splenium of the corpus callosum in adult male and female rats. Brain Res Dev Brain Res. 2000; 120:87–90. [PubMed: 10727734]

37. Ge Y, Grossman RI, Babb JS, et al. Age-related total gray matter and white matter changes in normal adult brain. Part I: volumetric MR imaging analysis. AJNR Am J Neuroradiol. 2002; 23:1327–1333. [PubMed: 12223373]

38. Lasiene J, Matsui A, Sawa Y, et al. Age-related myelin dynamics revealed by increased oligodendrogenesis and short internodes. Aging Cell. 2009; 8:201–213. [PubMed: 19338498]

39. Yuan J, Wang JZ, Lo S, et al. Hypofractionation regimens for stereotactic radiotherapy for large brain tumors. Int J Radiat Oncol Biol Phys. 2008; 72:390–397. [PubMed: 18374501]

40. Aoki M, Abe Y, Hatayama Y, et al. Clinical outcome of hypofractionated conventional conformation radiotherapy for patients with single and no more than three metastatic brain tumors, with noninvasive fixation of the skull without whole brain irradiation. Int J Radiat Oncol Biol Phys. 2006; 64:414–418. [PubMed: 16271441]

41. Aoyama H, Shirato H, Onimaru R, et al. Hypofractionated stereotactic radiotherapy alone without whole-brain irradiation for patients with solitary and oligo brain metastasis using noninvasive fixation of the skull. Int J Radiat Oncol Biol Phys. 2003; 56:793–800. [PubMed: 12788187]
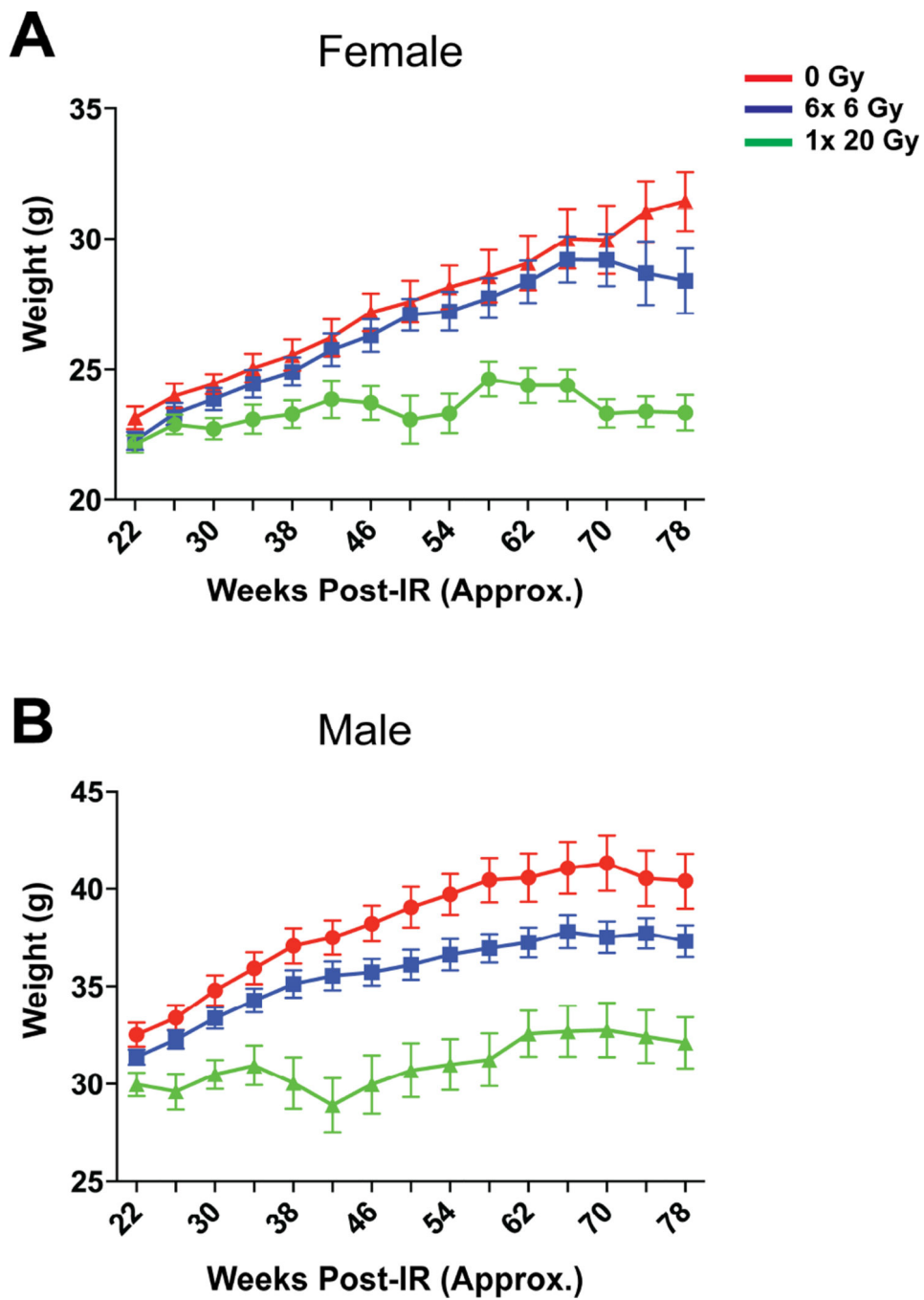
Fig. 1.
Weight gain in single and fractionated dose mice. Radiation and time from exposure significantly affect weight for both (A) female (p=0.0004 and p<0.0001, respectively) and (B) male (p<0.0001 for both) mice. n=13–20/group, 2-way ANOVA with repeated measures. Mean ± SEM shown.
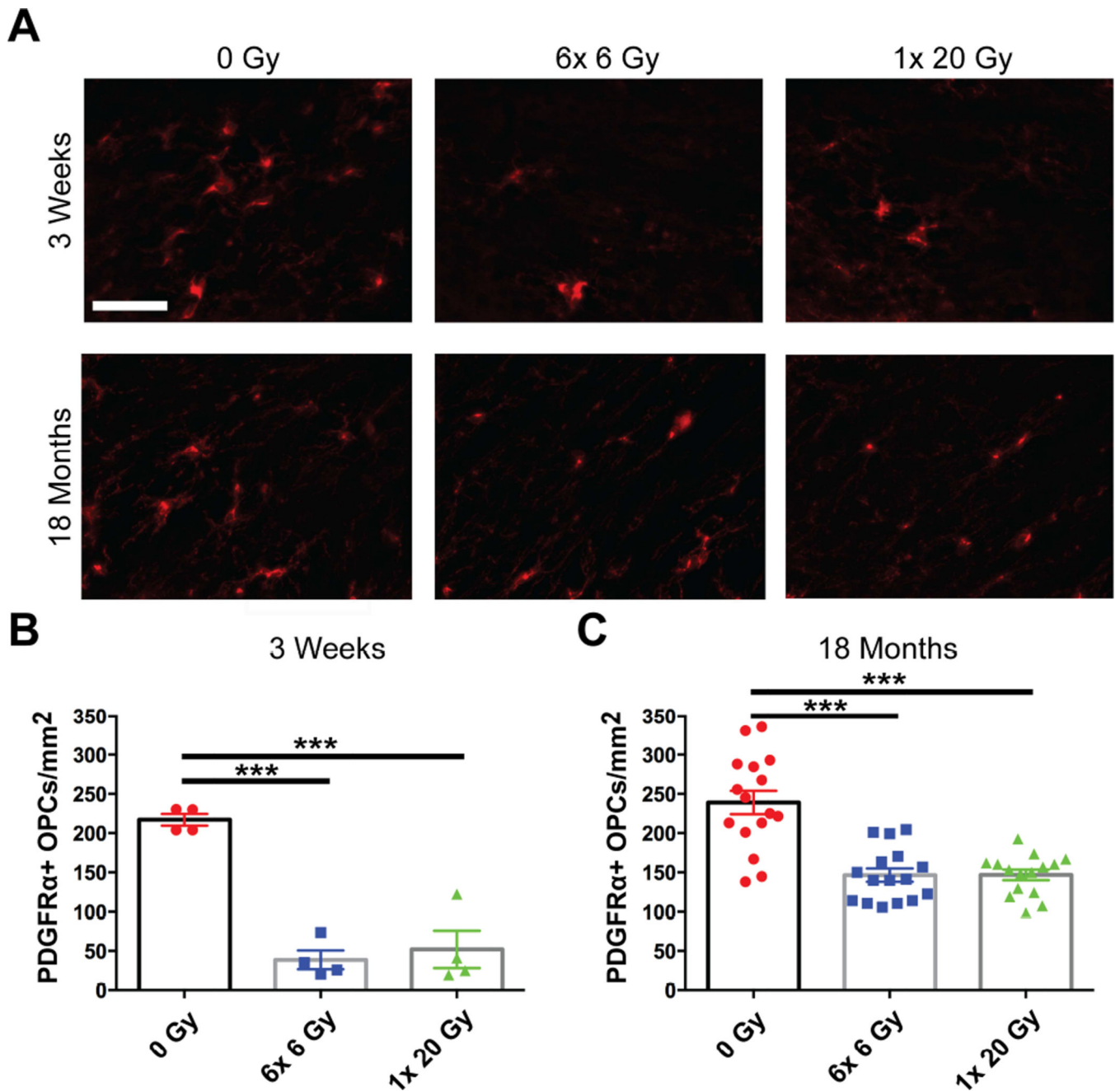
Fig. 2.

Fractionated and single dose IR result in early and delayed loss of OPCs. (A) Representative images show PDGFRα+ OPCs in the corpus callosum at 3 weeks and 18 months after 0 Gy, 6× 6 Gy, or 1× 20 Gy radiation exposure. Scale bar=10 μm. Radiation induced OPC loss at (B) 3 weeks and (C) 18 months (p<0.0001 for both). n=4–16 animals/group, 1-way ANOVA with Dunnett's multiple comparisons test. Mean ± SEM shown; ***p<0.001.
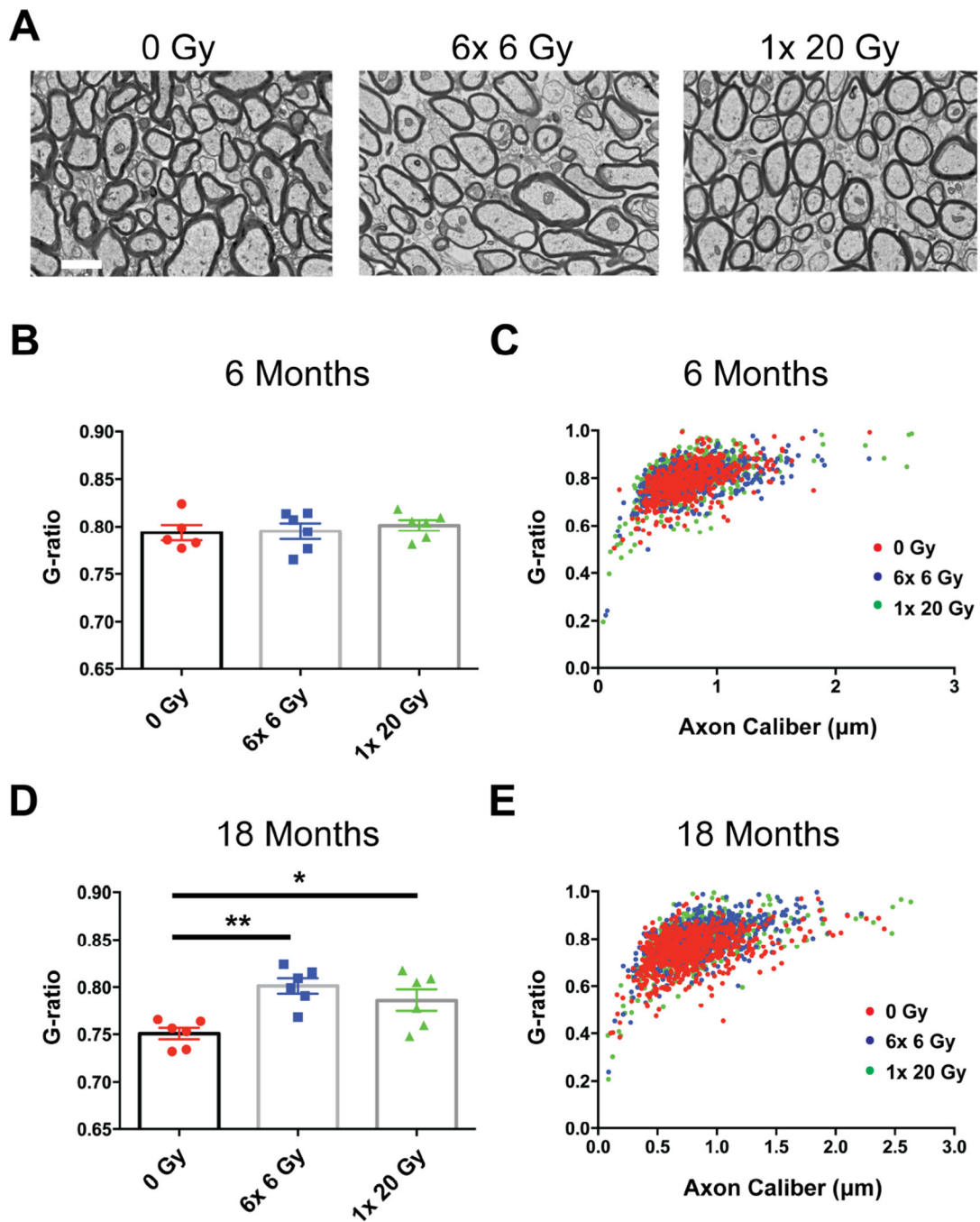
Fig. 3.

Myelin g-ratio is increased at 18 months in a size-dependent manner following cranial radiation. (A) Representative corpus callosum cross-sections 18 months after 0 Gy, 6× 6 Gy, or 1× 20 Gy radiation exposure. Scale bar=1 μm. (B) No significant change in average g-ratios 6 months after radiation exposure. (C) Scatter-graph showing g-ratios at 6 months as functions of axon caliber. There is excellent overlap among all 3 categories. (D) There is a significant increase in the average g-ratios of irradiated groups compared to controls at 18 months from exposure. (E) Scatter-graph at 18 months. The increase in g-ratio is confined to

the large caliber axons. n=5–6/group. 1-way ANOVA with Dunnett's multiple comparisons test. Mean ± SEM shown; *p<0.05, **p<0.01.
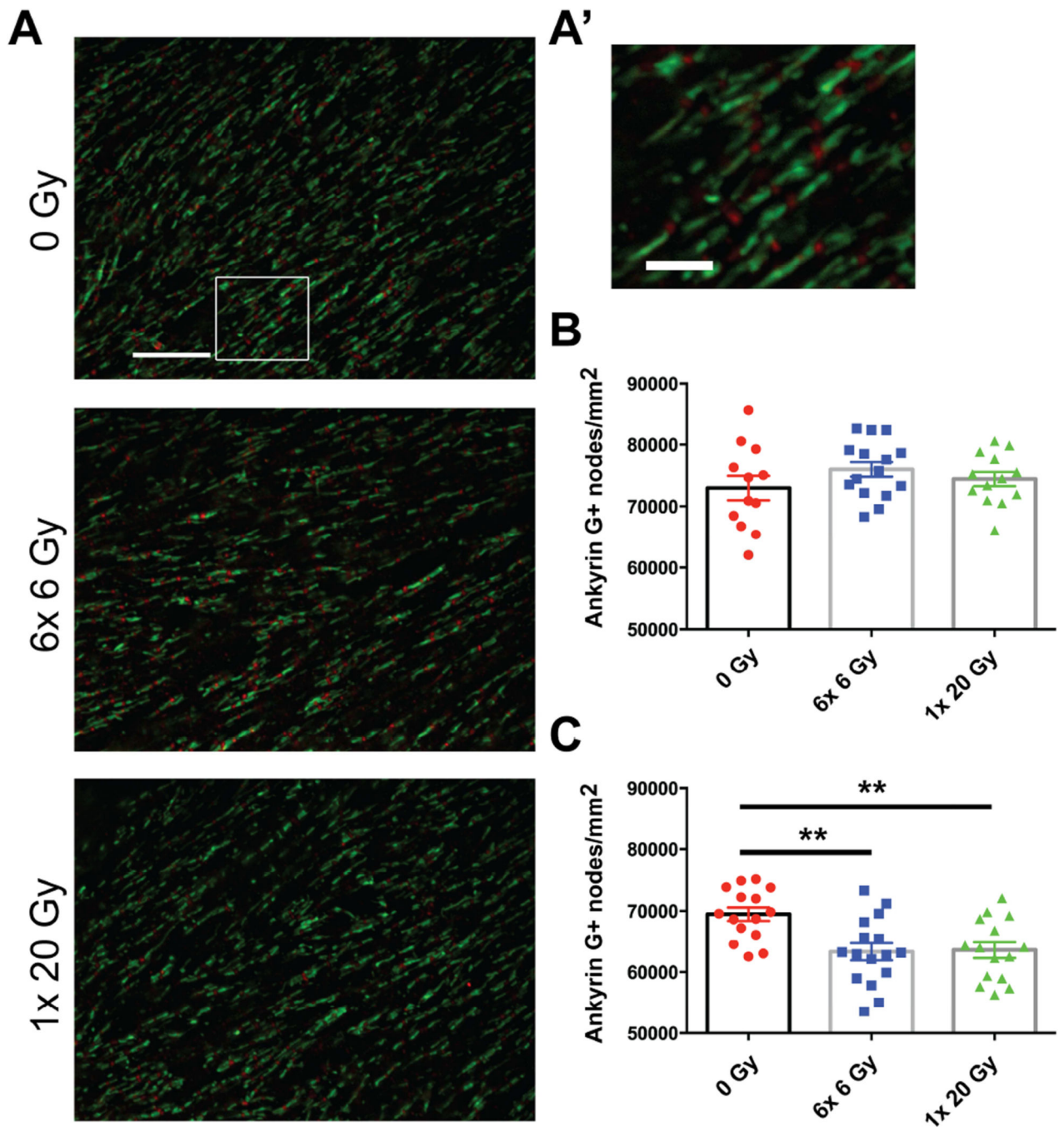
Fig. 4.
Nodes of Ranvier were reduced 18 months following radiation exposure. (A) Representative images show Ankyrin G (red) and Caspr (green) staining 18 months after 0 Gy, 6× 6 Gy, and 1× 20 Gy irradiation. Scale bar=3 μm. (A') Inset scalebar=1 μm. (C) Radiation significantly reduced Ankyrin G+ node density at 18 months (p=0.0016), but not (B) 6 months (p=0.3398). n=12–16/group. 1-way ANOVA with Dunnett's multiple comparisons test. Mean ± SEM shown; **p<0.01.
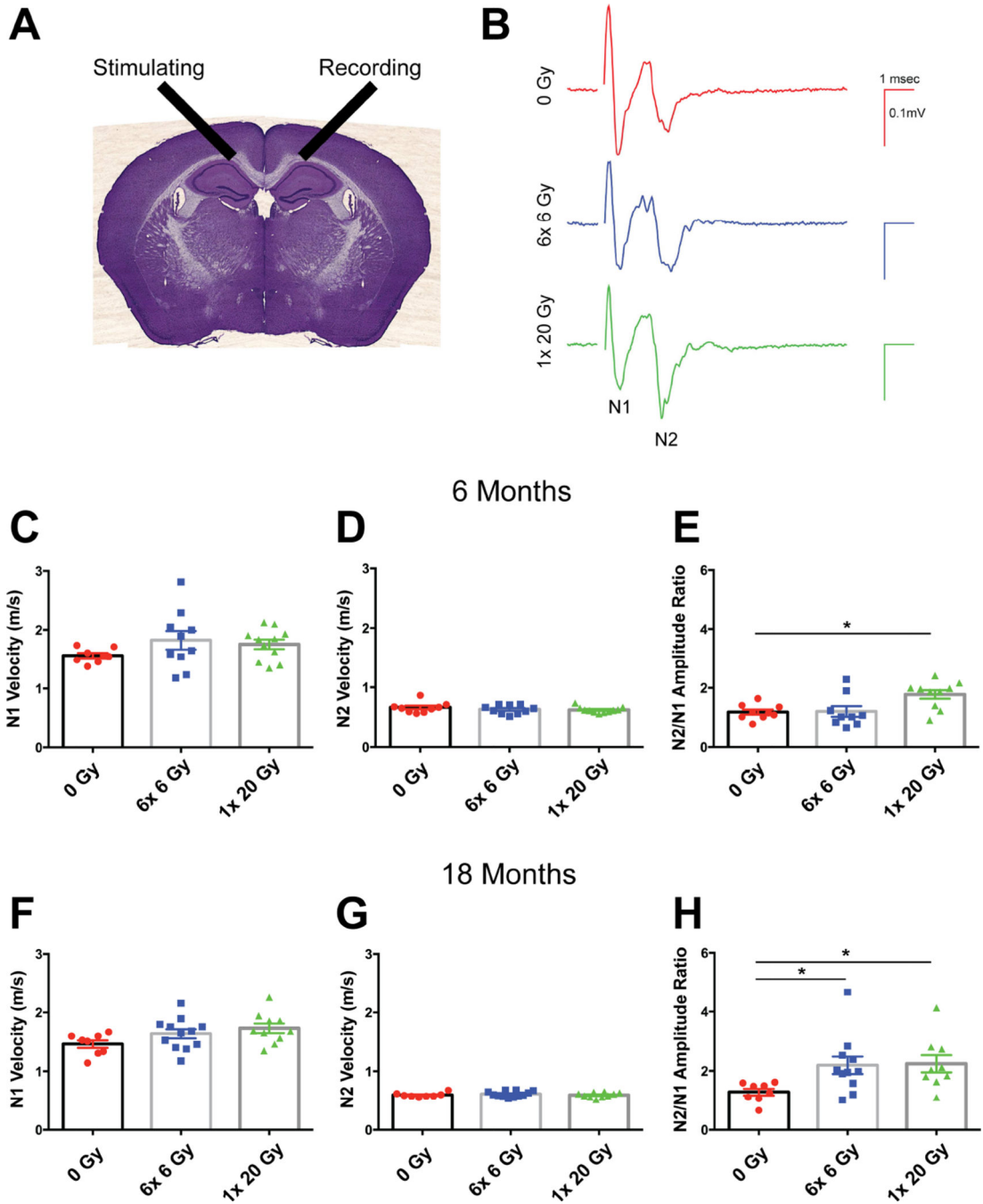
Fig. 5.
Radiation alters the ratio of small, unmyelinated fibers to large, myelinated fibers. (A) Interhemispheric conduction across the corpus callosum was assessed electrophysiologically. (B) Representative recordings taken 18 months after 0 Gy, 6× 6 Gy, and 1× 20 Gy radiation. Velocities were calculated from measured distances and the time to the N1 and N2 peaks. The ratio of N2/N1 amplitudes was calculated. (C, D, F, G) No difference in conduction velocity was seen with either radiation paradigm in either fiber type. The N2/N1 amplitude was increased at (E) 6 months (p=0.0202) and (H) 18 months

(p=0.0091) from radiation exposure. n=8–12/group. Data in C, D, E, G, H was analyzed by Kruskal Wallis test with Dunn's multiple comparisons test; 1-way ANOVA was used in F. Mean ± SEM shown; *p<0.05, **p<0.01.